Improved tip-tilt correction with ALTAIR, the Gemini North AO system

Jean-Pierre Véran, Glen Herriot, Les Saddlemyer, Keith Yeung
Herzberg Institute of Astrophysics
5071 West Saanich Road
Victoria B.C. V8X 4M6, Canada
Email: firstname.lastname@hia.nrc.ca

Abstract

Although tip-tilt may seem straightforward to correct with a high-order adaptive optics system, tip-tilt errors due to latency in the correction loop usually turn out to dominate the residual wave-fronts in the classical control scheme using a one integrator compensator and a fast tip-tilt mirror. In this paper, we propose a more sophisticated control scheme where the fast tip-tilt mirror as well as the deformable mirror and the telescope secondary mirror are used to corrected tip-tilt, with optimal use of their respective bandwidth and stroke. This scheme is based on a cascade of three integrators and is called multi-nested control loop. Its performance is assessed in the context of Altair, the future Gemini North high order adaptive optics system. It is found that in median observing conditions, this scheme allows to reduce the tip-tilt error rms by a factor of about 4, without significantly increasing the sensitivity of the control loop to wave-front sensing noise. In addition, it is found that these results can be achieve without requiring more than 1 Hz of bandwidth from the secondary mirror.

1 Introduction

Adaptive optics (AO) allows ground-based telescope to achieve diffraction limited resolution, but the correction is never perfect. Even with a bright guide source, one major limitation comes from the latency due to the wave-front sensor CCD read-out time and the wave-front reconstruction computing time. The goal of this paper is to investigate possible ways to overcome this effect. This study is quite general but is illustrated by the case of Gemini North and Altair, its future high order, Shack-Hartmann based, AO system. The parameters used to model this system and the typical observing conditions in which it will operate are described in section 2.

In classical observing conditions such as those at the top of Mauna Kea, and with a classical AO loop based on a one integrator compensator [3] it can be easily shown, as we do in section 3, that the correction errors due to latency are dominated by tip-tilt errors. This may sound surprising as it is well known that atmospheric tip-tilt is the slowest evolving aberration mode but can be explained by two reasons: firstly, the variance of tip-tilt in the incoming wave-front, which is generally due to both atmospheric turbulence and telescope wind-shake, is much higher than the combined variance of all the other aberrations modes. Tip-tilt correction errors result from the single integrator being unable to provide enough rejection considering that the latency force to operate the AO loop at reduced gain. Secondly, although the deformable mirror (DM) can correct for tip-tilt, its stroke is too small to handle such a huge variance and a specific device, a fast tip-tilt mirror (TTM), is generally used. This mirror has indeed the required stroke but is actually slower than the DM, which further increases the global loop latency.

Various schemes to beat down the effect of the loop latency have been proposed. They all come down to replacing the integrator by more sophisticated compensators, including a Smith compensator [3], a double integrator with lead filtering [8] and an optimised multi-step predictor [13] [4]. These schemes however makes use of only one device, that is the TTM for tip-tilt correction. But as we show in section 4, the deformable mirror, in addition to correcting for high order modes (defocus and up), could handle a fair amount of tip-tilt, at a potentially higher speed, without risk of saturation. This available dynamic on the DM can be used to correct for the fastest tip-tilt fluctuations whereas the slowest ones can be off-loaded to the telescope secondary mirror (M2), with the effect of decreasing the TTM dynamic and thus improving its mechanical performance and delivered image quality. This is exactly what the *multi-nested control loop* scheme that we propose in section 5 does. In this scheme, the actual frequency selection

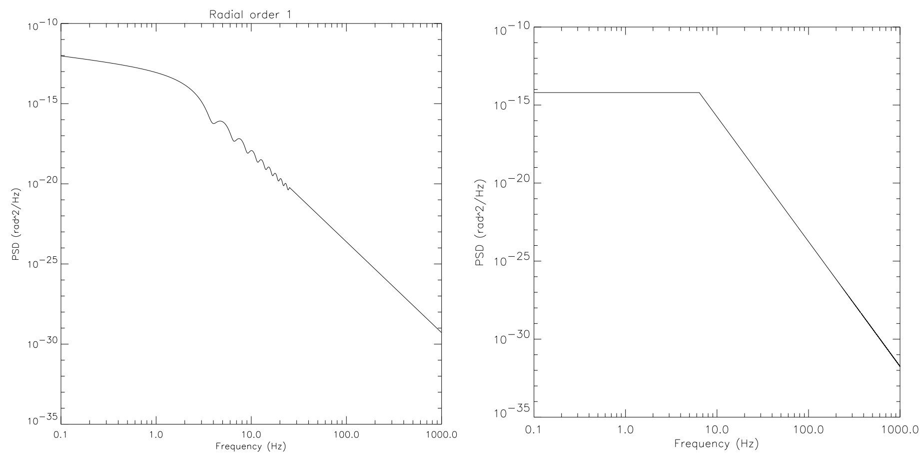

Figure 1: Power spectrum of the atmospheric tilt (left) and telescope wind-shake (right). The vertical scale represents the variance of the wave-front angle of arrival expressed in radians.

is performed by a cascade of three integrators, which has the effect of greatly increasing the tip-tilt rejection at low frequencies, without significantly increasing the over-shoot at high frequency, that is the sensitivity of loop to noise. One parameter of importance is how much bandwidth should be required from M2, as a low bandwidth (1 Hz in the case of Gemini) is very desirable to avoid potential vibration couplings between M2 and the AO system. This problem is also investigated.

2 Models

The following parameters apply to Gemini North and Altair. They are used to evaluate the performance of the tip-tilt correction:

- Atmospheric turbulence: Kolmogorov frozen turbulence consisting of one layer with $r_0 = 23.5\ cm$ @ 0.5 (zenith pointing) translating at $v = 20\ m/s$. The temporal power spectrum of the tilt computed from [2] is given in figure 1 left. The total integrated atmospheric tilt is 0.104 $arcsec\ rms$ and scale as $(D/r_0)^{5/6}$.
- Telescope wind-shake: Tilt perpendicular to the dome slit. Flat power spectrum with a 6.4 Hz cut-off frequency (see figure 1 right), corresponding to a local wind of $v = 8.4\ m/s$ [10], and giving a tilt of 0.0442 $arcsec\ rms$.
- Control loop: sampling frequency $F = 1\ kHz$, latency $\tau = 700\ \mu s$
- Deformable mirror: Perfect temporal response and a linear stroke of $\pm 4.2\ \mu m$ of wave-front correction (modelled after the Xinetics DM [12]).
- Tip-tilt mirror: Temporal response modelled after Thermotrex TTM [6], large stroke.
- Secondary mirror: 17 Hz closed-loop bandwidth when used in the 200 Hz Gemini Acquisition and Guidance (A&G) loop. From these specifications, the actual transfer function of M2 can be estimated [14]. Altair can take over the A&G loop and commands can be sent to M2 with a synchro delay of $t_{sync} = 400\ \mu s$ [9]. Very large stroke.

3 The simple control loop

Figure 2 sketches the principles of a generic AO loop, as described in detail in [3]: the wave-front computer (WFC) reads measurements from the wave-front sensor (WFS) and reconstruct the current wave-front error. A digital compensator (Comp) and a digital-to-analog converter are then used to update the wave-front correcting device

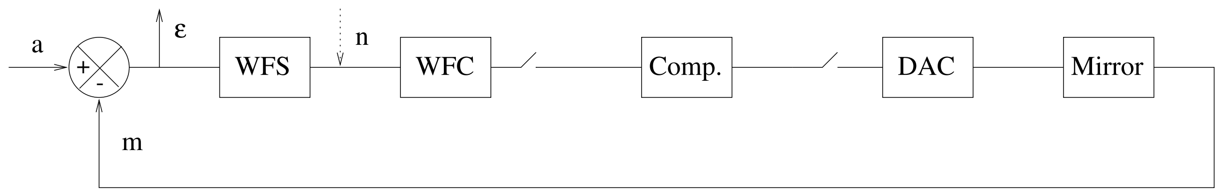

Figure 2: Diagram of a simple AO control loop.

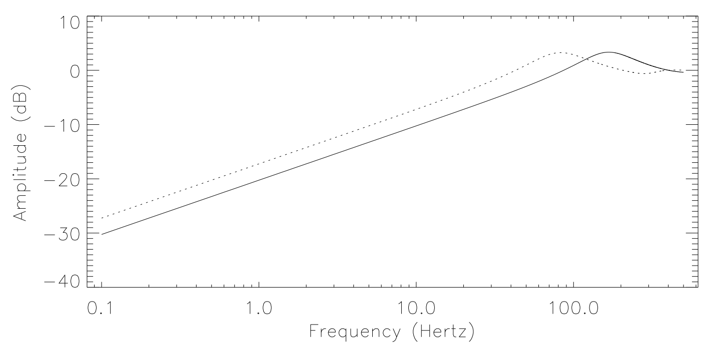

Figure 3: Simple loop correction transfer function for $F = 1000\ Hz$ and $\tau = 7\ ms$ using DM (solid line) or TTM (dotted line).

(Mirror). In this approach, modal control [7] [5], where each aberration mode is controlled by an independent scalar loop is implicitly assumed. The temporal performance of the system is characterised by the open-loop transfer function, expressed in the Laplace domain as: $H_{ol}(s) = \varepsilon(s)/m(s)$ which can be computed from the characteristics of each element of the loop [3]. The correction transfer function: $H_{cor} = \varepsilon(s)/a(s) = 1/(1 + H_{ol}(s))$ is the actual transfer function which is applied to the input spectrum when the system is working in closed-loop.

In most AO systems, the compensator is a simple integrator with a variable gain. The gain must be small enough to insure stability of the system. We impose stability by requiring the overall open-loop transfer function to have a 45 degree phase margin at the 0 dB gain point and a 6 dB gain margin at the -180 degrees phase point. These are classical criteria from control theory. Because the DM is faster than the TTM and therefore introduces less dephasing at high frequency, the loop with Mirror = DM can have a higher gain and therefore a better rejection at all frequency than the loop with Mirror = TTM. This is reflected by figure 3 where the two corresponding correction transfer functions are plotted.

For the correction of high order modes (defocus and up), the DM loop has to be used. In the turbulence conditions defined in section 2, the correction of Zernike Z_4 (defocus) to Zernike Z_{105} (which is assumed to be the maximal order of correction available from the DM) gives a residual wave-front error of 15 $\mu m\ rms$. The correction of tip-tilt (atmospheric turbulence + wind-shake) with the same DM loop gives a residual wave-front error of 19.5 $nm\ rms$ (18.1 nm for wind-shake and 7.3 nm for atmospheric tip-tilt). In this case though, the DM would saturate (see below). If instead we use the TTM in the simple loop, the contribution of the tip-tilt errors to the residual wave-front goes up to 38.7 nm (35.9 nm for wind-shake and 14.4 nm for atmospheric tip-tilt). This demonstrates that with a one integrator simple loop, tip-tilt errors due to loop latency strongly dominate in the residual wave-front.

r_0 @ 0.5 μm	23.5 cm	19.1 cm
$\delta_{HO\ turb\ edge}$	0.47 μm	0.56 μm
$\delta_{tilt\ edge}$ (allowed with 5σ margin)	0.70 μm	0.63 μm
rms tilt allowed on DM (angle of arrival)	0.036″	0.033″
rms total incoming tilt (Kolmogorov + wind-shake)	0.113″	0.132″

Table 1: amount of tip-tilt allowed on the DM without saturation, for a total actuator stroke of $\pm 4.2\ \mu m$ of wave-front correction.

4 Tip-tilt correction with the DM

The DM can easily produce tip-tilt. Since the DM has also an ideal time response, we would like to use it to correct for tip-tilt as well as for higher modes. Unfortunately, the stroke of the DM is too small to correct for the full incoming tip-tilt. But it can correct part of it. The goal of this section is to find out how much.

Since the incoming wave-front disturbance is dominated by tip-tilt, the largest wave-front excursions occur at the edge of the pupil. If the full wave-front is to be corrected by the DM only, saturation, if any, will occur at those actuators on the edge of the pupil. We want to avoid saturation at all cost.

For turbulent Kolmogorov wave-fronts, the rms excursion at the edge of the pupil when just the piston mode is corrected is [1]:

$$\delta_{turb\ edge} = \sqrt{1.90}\left(\frac{D}{r_0(\lambda)}\right)^{5/6}\frac{\lambda}{2\pi} \tag{1}$$

The variance of the Zernike tilt is given by Noll [11] as: $\sigma^2_{a_2} = 0.45(D/r_0)^{5/3}$. It follows that the rms contribution of the tilt to the wave-front excursion at the edge of the pupil is:

$$\delta_{tilt\ turb\ edge} = \sqrt{1.80}\left(\frac{D}{r_0(\lambda)}\right)^{5/6}\frac{\lambda}{2\pi} \tag{2}$$

It then follows that the rms contribution of the high-order (non-tilt) modes is:

$$\delta_{HO\ turb\ edge} = \sqrt{0.10}\left(\frac{D}{r_0(\lambda)}\right)^{5/6}\frac{\lambda}{2\pi} \tag{3}$$

Table 1 shows that with a 5σ saturation margin, the DM could handle more than 0.03 $arcsec$ rms of tip-tilt, that is 5 times the rms excursion required by the edge actuators to correct for the defocus and up plus that 0.03 $arcsec$ rms of tip-tilt is less than the total stroke of this actuator.

5 The multi-nested correction loop for tip-tilt

5.1 Description

Our proposed MNCL scheme for tip-tilt correction is sketched in figure 4. The MNCL can be seen as a simple loop similar to figure 2 but with a more sophisticated compensator based on a cascades of integrators (Integ). g_{DM}, g_{TTM}, g_N and g_{M2} are scalar gains whose value can be adjusted.

When $g_{DM} = g_N = g_{M2} = 0$, the MNCL is equivalent to the simple correction loop with the TTM, as described in section 2. Tip-tilt commands can be sent to the DM by increasing g_{DM}. But of course g_{DM} should be kept small enough so that the DM does not saturate. The frequency selection mechanisim (high frequencies on DM, low frequencies on TTM, very low frequncies on M2) is provided by additional integrators in the TTM path and in the

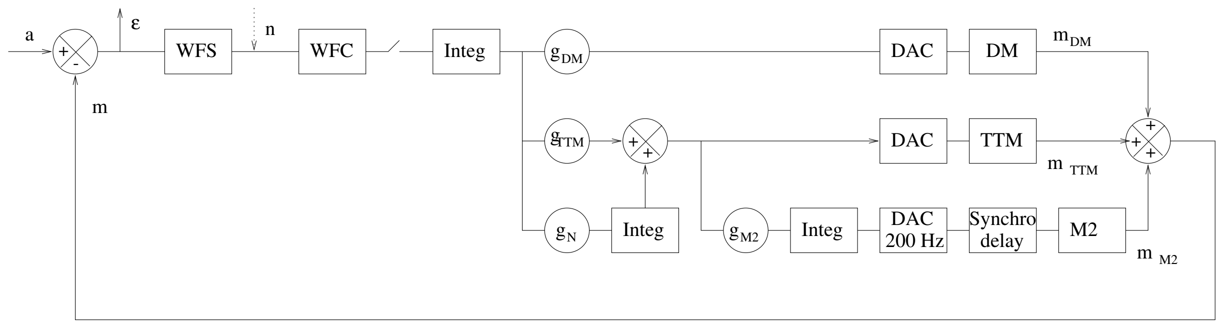

Figure 4: Diagram of the multi-nested AO control loop

	TTM only	TTM +DM	TTM+DM +M2(1Hz)	TTM+DM +M2(7Hz)
Corrected TT rms (nm)	39.7	9.10	10.21	8.80
TT stroke on DM rms (")	0.000	0.013	0.010	0.006
TT stroke on TTM rms (")	0.114	0.113	0.055	0.024
TT stroke on M2 rms (")	0.000	0.000	0.101	0.113
Total TT stroke rms (")	0.114	0.114	0.116	0.116
Noise amplification	0.008	0.011	0.009	0.009

Table 2: Performance of tip-tilt correction for various control schemes.

M2 path. The actual frequency splitting is defined by the choice of g_N and g_{M2} values. In particular, the higher g_{M2} the higher the frequency of the signal sent to M2.

In order to work properly, the MNCL must satisfy the stability criteria given in section 3. Our approach is to set g_{DM}, g_N and g_{M2} and optimise g_{TTM} so that the stability conditions are met. The multi-integration process tends to compromise the stability of the closed-loop though. Indeed, each integrator introduces a phase lag of -90 degrees. In order to retain a sufficient phase margin at the 0 dB gain point, the gains of the extra-integrators (g_N and g_{M2}) must be small enough compared to the gains of the direct paths (g_{DM} and g_{TTM}) so that the effects of these extra-integrators become negligible in the vicinity of the 0 dB critical point. In particular, this condition imposes $g_{M2} \leq 0.05$ and $g_N \leq 0.05$. Now, setting $g_{M2} = 0.05$ limits the signal sent to M2 to 7 Hz. In other words, if we try to send signals with frequency higher than 7 Hz, M2 starts fighting with the TTM and the DM and the loop becomes unstable. We conclude that *in our proposed scheme, M2 does not need a bandwidth higher than* 7 Hz. Finally, it is worth noting that the direct TTM path (through g_{TTM}) insures that a stable, saturation-free setting is always possible.

5.2 Performance

A systematic exploration of the (g_{DM},g_N,g_{M2}) space allowed us to select optimal settings. The results are reported in table 2. The setting of interest are the following:

- *TTM only*: $g_{DM} = g_N = g_{M2} = 0$. This is the simple control loop using only the TTM to correct for tip-tilt, as studied in section 3.
- *TTM + DM*: $g_{DM} = 0.54$, $g_N = 0.05$ $g_{M2} = 0$: This is a simple nested loop where $M2$ is not used at all.
- *TTM + DM + M2(1Hz)*: $g_{DM} = 0.54$, $g_N = 0.05$ $g_{M2} = 0.0065$: This is a multi-nested loop where M2 is used with a bandwidth of 1 Hz only.
- *TTM + DM + M2(7Hz)*: $g_{DM} = 0.54$, $g_N = 0.05$ $g_{M2} = 0.05$: This is a multi-nested loop where M2 is used with a bandwidth of 7 Hz.

The results are:

- *Corrected TT rms (nm)*: the overall tip-tilt correction error expressed in nanometers rms of wave-front. This number can be fed directly into the AO system's error budget.
- *TT stroke on DM rms (")*: how much tip-tilt is handled by the DM, expressed in arc-seconds rms.
- *TT stroke on TTM rms (")*: how much tip-tilt is handled by the DM, expressed in arc-seconds rms.
- *TT stroke on M2 rms (")*: how much tip-tilt is handled by the DM, expressed in arc-seconds rms.
- *Total TT stroke rms (")*: the total TT correction, expressed in arc-seconds rms. This is the quadratic sum of the three numbers above.
- *Noise amplification*: the square root of the integral of the noise transfer function, defined as $H_n(s) = m(s)/n(s)$ for $a = 0$. This number quantifies how sensitive to noise the loop is.

Examination of table 2 leads to the following comments:

- Using the DM to correct part of the tip-tilt reduces the rms tip-tilt error by about a factor 4, which is a very significant gain, making the correction errors on tip-tilt comparable to the correction errors on higher modes.
- Using the DM to correct part of the tip-tilt does not significantly increase the noise sensitivity of the control loop.
- The amount of tip-tilt that must be handled by the DM is well below 0.03 $arcsec\ rms$, which is the maximum value defined in section 3.
- Using M2 reduces the amount of tip-tilt to be handled by the DM and the TTM. This is desirable, for optical and mechanical reasons.
- Using M2 at the highest frequency reinforces the above effect. The difference however does not seem to justify the risk of operating M2 at 7 Hz instead of 1 Hz.

We thus conclude that a multi-nested correction loop for tip-tilt is really beneficial and that there is no real need to operate $M2$ faster than 1 Hz.

In order to get further insight on how the MNCL works, results obtained for the M2 at 1 Hz setting ($g_{M2} = 0.0065$), for different values of g_{DM} and g_{TTM} are plotted in figure 5. It shows that increasing g_N both reduces the residual error and the noise amplification coefficient as well as, of course, the dynamic range of the DM. But for high g_N, g_{DM} must be higher than a certain threshold in order to insure stability. Since the noise propagation coefficient increases with g_{DM} but decreases with g_N, the optimal setting is the highest possible g_N (that is 0.05 here) and for this value the lowest possible g_{DM}. Hence the choice above of the settings: $g_{DM} = 0.54$, $g_N = 0.05$ $g_{M2} = 0.0065$. As a more practical illustration of how the system behaves, figure 6 shows the response of each device to a step input. The frequency selection effect appears clearly: the step is immediately compensated by the DM. Very soon after, the TTM takes over. Then the correction is slowly transfered from the TTM to M2.

6 Conclusion

In this article, we have described a new scheme for tip-tilt correction called the multi-nested correction loop, that is able to significantly decrease the wave-front correction error due to loop latency, without significantly increasing the sensitivity of the loop to wave-front sensing noise. This scheme is general but has been designed and tested for Altair, the Gemini North adaptive optics system. This scheme uses an easy-to-implement cascade of three integrators that makes optimal use of the different devices able to correct for tip-tilt, namely the deformable mirror, the tip-tilt mirror, and the telescope secondary mirror. This allows a reduction of the rms residual tip-tilt error by about a factor 4, which is a very important gain. The study also shows that in this scheme, the secondary mirror shall never be used at a bandwidth higher than 7 Hz and that a bandwidth of 1 Hz is very satisfactory.

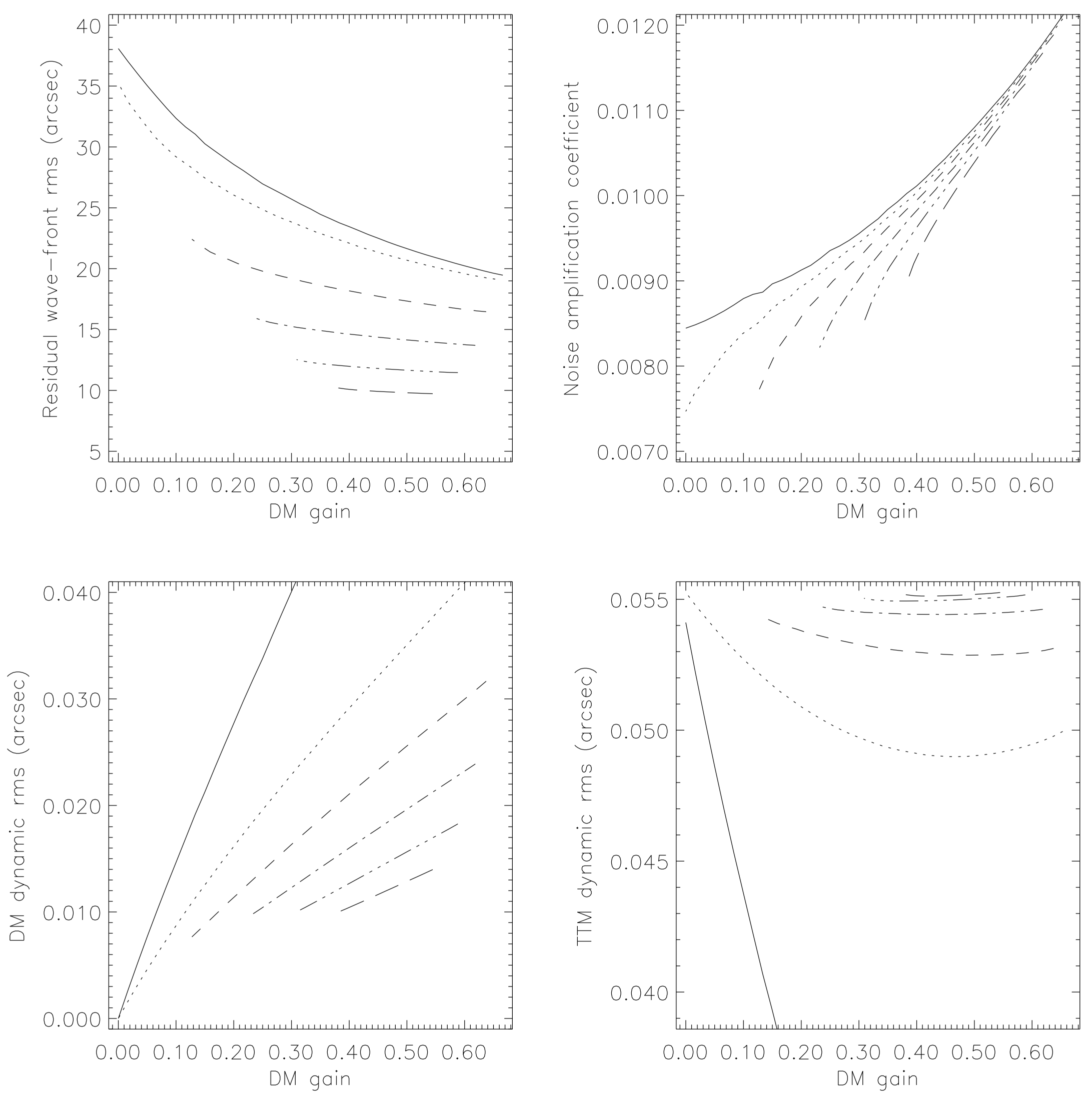

Figure 5: Tip-tilt (atmospheric + windshake) correction performance as a function of g_{DM} for $g_{M2} = 0.0065$ and for $g_N = 0$ (solid line), $g_N = 0.01$ (dotted line), $g_N = 0.02$ (dashed line), $g_N = 0.03$ (dash dot), $g_N = 0.04$ (dash dot dot dot) and $g_N = 0.05$ (long dashes). g_{TTM} is optimised for stability.

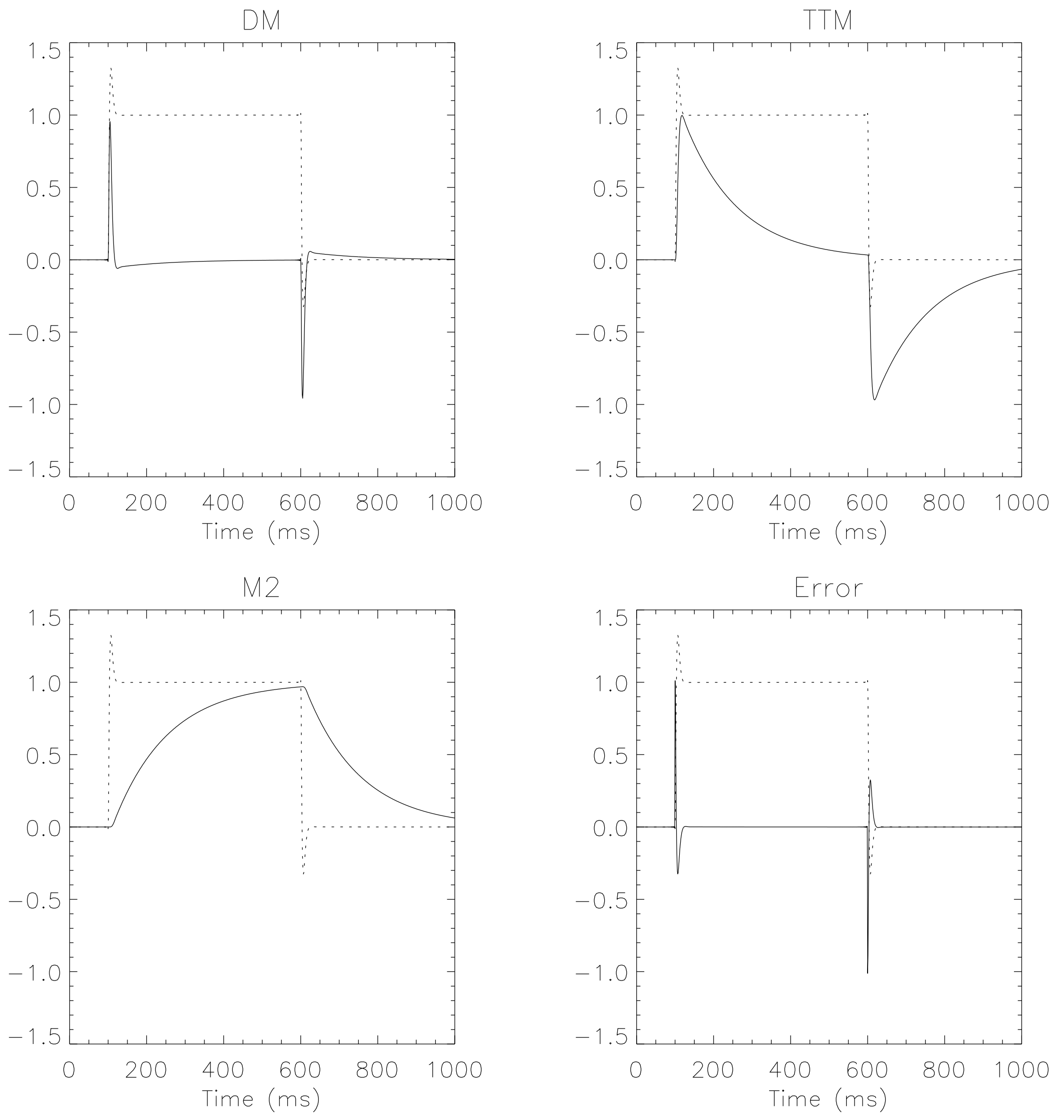

Figure 6: Response of DM, TTM and M2 to a rectangular disturbance spanning from $t = 100ms$ to $t = 600ms$ for $g_{DM} = 0.54$, $g_N = 0.05$, $g_{M2} = 0.0065$ and g_{TTM} optimised for stability. Dotted line is the total TT correction provided by the system and the error plot (bottom right) shows the difference between this correction and the actual input.

7 Acknowledgements

We would like to express our gratitude to Jean-Marc Conan for kindly providing us with pre-computed tilt spectra, and to Brian Leckie for his interest and advices.

References

[1] J.-M. Conan. *Étude de la correction partielle en optique adaptative.* PhD thesis, Université Paris XI, Orsay, France, 1994.

[2] J.-M. Conan, G. Rousset, and P.-Y. Madec. Wave-front temporal spectra in high-resolution imaging through turbulence. *J. Opt. Soc. Am. A*, 12(7):1559–1570, 1995.

[3] M. Demerlé, P.Y. Madec, and G. Rousset. Servo-loop analysis for adaptive optics. In D. M. Alloin and J.-M. Mariotti, editors, *Adaptive Optics for Astronomy*, volume 423 of *NATO Advanced Science Institutes Series*, pages 73–88. Kluwer Academic Publishers, 1994.

[4] C. Dessenne, P.-Y. Madec, and G. Rousset. Optimization of a predictive controller for closed-loop adaptive optics. *Appl. Opt.*, 37(21):4633–4633, 1998.

[5] B.L. Ellerbroek, C. Van Loan, N.P. Pitsianis, and R.J. Plemmons. Optimizing closed-loop adaptive-optics performance with use of multiple control bandwidths. *J. Opt. Soc. Am. A*, 11(11):2871–2886, nov 1994.

[6] J. Farinato, S. Esposito, E. Marchetti, R. Ragazzoni, and D. Bruns. Performance of a magnetic driven Tip-Tilt mirror. In A. Ardeberg, editor, *Optical Telescopes of Today and Tomorrow*, volume 2871 of *Proc. SPIE*, pages 962–968, 1996.

[7] E. Gendron and P. Léna. Astronomical adaptive optics I. Modal control optimization. *Astron. Astrophys.*, 291:337–347, 1994.

[8] S. Hippler, A. Glindemann, M. Kasper, P. Kalas, R.-R. Rohloff, K. Wagner, D. P. Looze, and W. Hackenberg. ALPHA: The MPIA/MPE adaptive optics with a laser for astronomy project. In D. Bonaccini and R. K. Tyson, editors, *Adaptive Optical System Technologies*, volume 3353 of *Proc. SPIE*, pages 44–55, 1998.

[9] R. McGonegal. Fast tip/tilt loop latency. Interface Control Document G0012, International Gemini Project Office, 28 June 1995.

[10] R. McGonegal. Wind spectra for gemini. Memo, International Gemini Project Office, 30 Dec 1996.

[11] R.-J. Noll. Zernike polynomials and atmospheric turbulence. *J. Opt. Soc. Am.*, 66(3):207–211, 1976.

[12] B.R. Oppenheimer. Investigating a Xinetics deformable mirror. *Proc. SPIE*, 3126:569, 1997.

[13] W. Wild. Innovative wavefront estimators for zonal adaptive optics. *Proc. SPIE*, 3126:278–287, 1997.

[14] K. Yeung. Servo analysis for the M2 T/T/F correction. Altair: preliminary design review documents, NRC Canada, Oct 1997.